Classification of Large-Scale Environments that drive the formation of Mesoscale Convective Systems over Southern West Africa

Francis Nkrumah[1,2], Cornelia Klein[3,5], Kwesi Akumenyi Quagraine[1,4], Rebecca Berkoh Oforiwaa[2,6], Nana Ama Browne Klutse[2,6], Patrick Essien[1,2], Gandomè Mayeul Leger Davy Quenum[2,7] and Hubert Azoda Koffi[6]

[1]Department of Physics, University of Cape Coast, Private Mail Bag, Cape Coast, Ghana;
[2]African Institute of Mathematical Sciences (AIMS), Sector Remera, Kigali 20093, Rwanda;
[3]U.K. Centre for Ecology and Hydrology, Wallingford, United Kingdom
[4]Climate System Analysis Group (CSAG), ENGEO, University of Cape Town, Private Bag X3, Rondebosch, Cape Town 7701, South Africa
[5]Department of Atmospheric and Cryospheric Sciences, University of Innsbruck, Innsbruck, Austria
[6]Department of Physics, University of Ghana, Legon P.O. Box LG 63, Ghana
[7]National Institute of Water (NIW), University of Abomey-Calavi, Godomey, Cotonou 01 PB: 4521, Benin

Correspondence to: Francis Nkrumah (francis.nkrumah@ucc.edu.gh) and Nana Ama Browne Klutse (nklutse@ug.edu.gh)

Abstract. Mesoscale convective systems (MCSs) are frequently observed over southern West Africa (SWA) throughout most of the year. However, it has not yet been identified what variations in typical large-scale environments of the West African monsoon seasonal cycle may favour MCS occurrence in this region. Here, six distinct synoptic states are identified and are further associated with being either a dry season, pre-, post-, or peak-monsoon synoptic circulation type using self organizing maps (SOMs) with inputs from reanalysis data. We identified a pronounced annual cycle of MCS numbers with frequency peaks in June and September ~~which~~that can be associated with peak rainfall during the major and minor rainy seasons respectively across SWA. Comparing daily MCS frequencies, MCSs are most likely to develop during post-monsoon conditions featuring a northward-displaced moisture anomaly (0.42 MCSs per day), which can be linked to strengthened low-level westerlies. Considering that these post-monsoon conditions occur predominantly from September and into November, these patterns may in some cases be representative of a delayed monsoon retreat. On the other hand, under peak monsoon conditions, we observe easterly wind anomalies during MCS days, which reduce moisture content over the Sahel but introduce more moisture over the coast. Finally, we find all MCS-day synoptic states to exhibit positive zonal wind shear anomalies. Seasons with the strongest zonal wind shear anomalies are associated with the strongest low-level temperature anomalies to the north of SWA, highlighting that a warmer Sahel can promote MCS-favourable conditions in SWA. These significant positive zonal wind shear anomalies for MCS days illustrate the importance of zonal wind shear for MCS development in SWA throughout the year.

1 Introduction

The region of West Africa is subject to variabilit~~iesy~~ in rainfall on both spatial and temporal scales. Fundamentally, the rainfall pattern in West Africa is modulated by the annual change in the position of the

Intertropical Convergence Zone (ITCZ) and the West African Monsoon (WAM). Due to endemic poverty, lack of infrastructure and technology, rapid population increase, and significant fluctuation of the WAM, West Africa has been deemed one of the world's most susceptible regions to climate change (~~Change~~IPCC, 2014). The climate of southern West Africa (SWA) can be categorized into four seasonal stages: a dry season from December to February, two wet seasons lasting from April to June, and September to November, and the so-called little dry season in August (e.g. Thorncroft et al. 2011). Between March and June, when low-level winds are more westerly and the intertropical convergence zone (ITCZ) starts to move northward, the precipitable water peaks over SWA (Klein et al. 2021). The ITCZ retreats southward in September, creating the second rainy season, followed by a dry season from November to January.

One ~~of the most destructive high-impact weather phenomena in West and Central Africa are mesoscale convective systems (MCSs), together with the precipitation, wind, and lightning they bring (Baidu et al. 2022).~~major atmospheric disturbance that contributes to the WAM is the presence of Mesoscale Convective Systems (MCSs) which supplies around 30-80 % of the total rainfall during the WAM (Klein et al. 2018). MCSs are organized thunderstorm clusters, often defined to have a minimum horizontal extent of the precipitating area of 100 kilometres in at least one direction (Guo et al. (2022); Chen et al. (2022); Houze (2004)). Maranan et al. (2018) note that diverse MCS sub-groups such as squall- or disturbance lines, structured convective systems, and mesoscale convective complexes impact the hydro-climate of West Africa. In both the tropics and midlatitudes, MCS also contributes significantly to rainfall extremes, rendering them a substantial contributor to the hydrologic cycle (Feng et al. (2021); Li et al. (2020)). More studies have been motivated in recent decades by evaluating drivers that affect rainfall variability and intensity associated with MCSs (Baidu et al. (2022); Augustin et al. (2022)). MCSs, for instance, supply essential precipitation and, as a result, supply water to agriculturally productive regions in the tropics, particularly in semi-arid regions such as the Sahel (Nesbitt et al. (2006)).

However, relative to our understanding of MCS drivers in the Sahel, SWA has received less attention. The connections of MCSs to larger-scale atmospheric motion and states are both important and not fully understood for the southern region, hence, a better understanding of large-scale MCS drivers is important for improving precipitation prediction over SWA. Earlier research has suggested an increasing role of other types of less-organized rainfall in place of MCSs over the Guinea Coast (e.g. (Acheampong, 1982; Fink et al., 2006; Kamara, 1986; Omotosho, 1985), with MCS contribution to annual rainfall decreasing from 71% in the Soudanian to 56% in the coastal zone (Maranan et al 2018), emphasizing MCS importance across the SWA region. Maranan et al., 2018 also concluded that precipitable water and Convective Available Potential Energy (CAPE) determine where MCSs may occur in SWA, while zonal wind shear is a stronger predictor for distinguishing between small scattered convection and MCS-type development. Indeed, zonal wind shear intensification was found to be a major driver of increasing frequencies of the most intense Sahelian MCSs over the last three decades (Taylor et al., 2017), a mechanism that was similarly found to play a role for early-season MCS intensification in SWA (Klein et al 2021). ~~W~~Zonal wind shear, which is thought to modulate the storm-available supply of moist buoyant air, is also seen to be very critical to the organization of convective systems (e.g., Alfaro, 2017; Mohr & Thorncroft, 2006). Accordingly, propagating storms with longer-lasting organized precipitation systems were consistently found to be associated with strong

vertical wind shear and higher values of CAPE in the Sahel (Hodges & Thorncroft, 1997; Laing et al., 2008; Mohr & Thorncroft, 2006).

~~In p~~Previous studies address the large-scale settings for WAM-related rainfall throughout the seasons~~that evaluated MCS-favouring atmospheric environments,~~ (Sultan and Janicot, 2003) with less attention ~~was~~ given to the importance of large-scale WAM modes and their effect on regional MCS frequencies in SWA. The role of regional MCS-centred environments in the initiation and development of MCSs in West Africa has been well studied (e.g., Klein et al. 2021; Vizy and Cook 2018; Schrage et al. 2006; Maranan et al. 2018). Vizy and Cook (2018) observed that the extension of vertical mixing to the level of free convection, as a result of surface heating, tends to initiate MCSs in an environment where the mid-tropospheric African easterly wave disturbance is located in the east. The vertical wind shear is enhanced as a result of the synoptic disturbance. Klein et al. (2021) suggested that heavy rainfall, due to cold MCSs during both dry and rainy seasons, occurs in an environment with stronger vertical wind shear, increased low-level humidity, and drier mid-levels. Unlike vertical wind shear, Maranan et al., (2018) suggested that thermodynamic conditions such as CAPE and Convective Inhibition (CIN) are of lesser importance for the horizontal growth of convective systems, although they indicate the potential of the initial vertical development of convective systems. Janiga and Thorncroft (2016) also suggested that CAPE, vertical wind shear and column relative humidity are the decisive large-scale environmental parameters~~s~~ that control the characteristics of convective systems. Based on radar and sounding observations aligned around 15°N, Guy et al. (2011) analyzed MCSs and their respective environmental conditions over three different regimes of West Africa (maritime, coastal, and continental). They concluded that MCSs tend to occur ahead of the African easterly wave (AEW) trough during the maritime and the continental regime, while they are mostly found behind the trough in the coastal regime.

It is not clear to what extent different large-scale patterns such as temperature, wind, humidity, and CAPE at different stages of the WAM drive the formation of MCSs over SWA. Hence, this study systematically classifies the different large-scale patterns across the WAM region and how they are associated with MCSs over SWA. For this purpose, a classification using a self organizing map (SOM; Kohonen 2001) analysis was carried out to characterize large-scale WAM patterns during the 1981-2020~~19~~ period, which we subsequently ~~stratify for~~grouped into days with MCS occurrence over SWA. The SOM is a clustering technique that is topologically sensitive and uses an unsupervised training method to cluster the training data (Lennard and Hegerl, 2014; Quagraine et al. 2019). This methodology thus allows us to identify favourable types of large-scale environments driving the formation of MCSs within different WAM stages.

The paper is organized as follows: Section 2 details the study area and data sources and how they were processed. In section 3, the SOM methodology and other needed statistics used to investigate the relationship between large-scale environment patterns and particular MCSs are presented. Section 4 discusses the main results, which include the common features and different types of large-scale patterns associated with MCSs. Section 5 provides the summarized conclusions of the study.

2 Data Sources and Processes

2.1 ERA5 Reanalysis Data and MCS Data

The ECMWF fifth-generation atmospheric reanalysis (Hersbach et al., 2020), ERA5, was used as the main ~~product~~data source in this work. The dataset is generated using 41r2 of the Integrated Forecast System (IFS) model, based on a four-dimensional variational data assimilation scheme, and takes advantage of 137 vertical model levels and a horizontal resolution of 0.28125° (31 km). The data provides hourly estimates of model integration. In this study, hourly zonal and meridional winds (650~~250~~ and 925 hPa), specific humidity (925 hPa), temperature (925 hPa), and convective available potential energy (CAPE) in ERA5 during 1981–2020 were used to explore suitable large-scale environments for the development of MCSs in SWA (5-9°N, 10°W-10°E). The zonal and meridional wind, as well as specific humidity at 925 hPa, are used to understand the penetration of monsoon flow inland. The zonal wind difference between 925 hPa and 650 hPa is used as a zonal wind shear change indicator while the temperature at 925 hPa is used to visualize Saharan heat low (SHL) differences.

The Meteosat Second Generation (MSG) cloud-top temperature data, which are available every 15 minutes from the Eumetsat archives online (https://navigator.eumetsat.int/product/EO:EUM:DAT:MSG:HRSEVIRI) was used in this study. ~~Twelve~~Fifteen years of MCS snapshots (2004–15~~8~~) detected from Meteosat Second Generation 10.8 μm-band brightness temperatures (Schmetz et al. 2002, EUMETSAT 2021) are used to define MCS days in this study. Following Klein et al. (2021), an MCS is defined here as a -50°C contiguous cloud area larger than 5000 km^2. An "MCS day" is then defined as a day with at least 5 MCS~~s snapshots~~ between 16 and 1900 UTC per day that is raining >5mm within the SWA domain. This can include the same MCS at several timesteps in a day. Corresponding rainfall snapshots were sampled from the ‘‘high-quality precipitation’’ (HQ) field within the Integrated Multi-satellite Retrievals for Global Precipitation Measurement (IMERG; Huffman et al. 2019) dataset. Here, only land-based MCSs because MCSs over land are fundamentally more intense and deep than its counterpart over the ocean (Mohr and Zipser 1996).

3 Methodology

3.1 Self-organising Maps (SOMs) analysis

The study uses the self organizing map (SOM; Kohonen 1982, 2001) from SOM-PAK-3.1 software. The technique is used to identify archetype synoptic circulation patterns over the southern West Africa region by training a 9-node SOM with ERA5 daily mean 925 hPa geopotential height fields to produce 9 characteristic circulation patterns for the period 1981 to 2020. The geopotential height circulation pattern is used here mainly based on its physically realistic output spanning a range of circulation features found in the atmosphere (Hewitson and Crane, 2002) and its ability to detect the West African Heat Low (WAHL) which ia a key element of the West African monsoon system (Lavaysse et al. 2009; Biasutti et al. 2009). ~~The SOM is a clustering technique that is topologically sensitive and uses an unsupervised training method to cluster the training data (Lennard and Hegerl, 2014; Quagraine et al. 2019). It~~The SOM is mostly the preferred choice over other clustering methods such as the principal component analysis (PCA) or K-means because the data is not discretized and orthogonality is not forced~~-~~ or does not require subjective rotations to produce interpretable patterns. The main advantage of the SOM technique is ts ability to deal with non-linear data (such as the continuum of atmospheric conditions) ~~but rather treats the data as a continuum~~and can easily be visualized and interpreted (Reusch et al. 2005; Lennard and Hegerl, 2014). The steps

within the technique can be broadly grouped into two stages, namely the training stage and the mapping stage. Earlier studies (e.g. Hewitson and Crane 2002; Kim and Seo 2016; Lee 2017; Rousi et al. 2015; Sheridan and Lee 2012) have successfully used this technique in synoptic climatology to effectively preserve relationships between weather states while giving outputs that are readily understood and can be easily visualized as an array of classified patterns. These classified patterns help in interpreting relationships between large-scale regional circulation patterns and local weather expressions and rainfall extremes (Hewitson and Crane 1996; Cassano et al. 2015; Wolski et al. 2018). In this study, the SOM is randomly initialized allowing for hidden patterns and structure in the geopotential height at 925 hPa to be discovered while the algorithm iteratively updates the weights of the nodes to better represent the data. The strength of initializing the SOM this way lies also on its robustness to noise and outliers as a result of the algorithm applying a competitive learning structure to the data which then allows for the formation of distinct clusters. The SOM_PAK algorithm allows the SOM process to minimize quantization and topological errors at the mapping stage when choosing the best SOM as outlined in Lennard and Hegerl (2014). However, t~~T~~here is a trade-off when choosing the size of the SOM, as this is dependent on the need to generalize circulation states for analyses or the need to capture predominant spatial characteristics that affect the local climate. Thus, in this study, we have tested several sizes of the SOM and have arrived at using a 9-node SOM. ~~The 9-node SOM is a compromise on states not being overly generalized while capturing the dominant spatial characteristics over the region.~~As depicted in Fig. S1 for a 9-node SOM, it is evident that some nodes are still redundant, and this is a compromise on states not being overly generalized while capturing the dominant spatial characteristics over the region. Here, we agree on six nodes, which allow distinct synoptic states to be reproduced while grouping nodes that are similar. This grouping was done based on similarities in atmospheric patterns and seasonal frequency from the 9-node case.

3.2 Large-scale WAM patterns on southern West Africa MCS days

Based on the ~~9~~6 different large-scale node patterns, we explore within-node large-scale conditions that characterize MCS days in SWA. For examination of environmental conditions suitable for SWA MCS activity, large-scale conditions were taken from hourly ERA5 reanalysis data sampled at 1200 UTC when the daily convective activity is more representative of pre-convective atmospheric conditions (Klein et al. 2021). Pre-convective conditions are considered in the study to reduce the effects of feedback from the MCSs on environmental conditions (Song et al. 2019). Composites of ERA5 large-scale environmental variables (temperature, wind, specific humidity, and CAPE) are created for all node days, and for MCS days within each SOM node. Finally, the anomaly in large-scale patterns between MCS days and node mean conditions are computed to determine MCS-favourable adjustments in large-scale patterns within each node. A two-sided Student's t-test is used to determine significant differences between node climatologies and MCS-day sub-samples.

In addition to large-scale condition composites, we also sample pre-convective (1200 UTC) local atmospheric conditions (ERA5), for each 1800 UTC MCS at the location of minimum cloud top temperature. We only consider 1800 UTC MCSs for local condition sampling to avoid oversampling similar atmospheric states from several MCS time steps. These conditions are compared to the node climatology conditions at the same locations,

allowing us to explore the difference in node climatology versus MCS day conditions at the specific locations where MCSs occurred on respective days.

4 Results

4.1 Node seasonality and mean conditions

In analyzing the 9-node SOM (~~not shown~~Fig. S1), six SOM nodes (Fig. 1) with distinct synoptic states were identified and were further associated with being either a pre-, post-, or peak-monsoon synoptic circulation type as a result of which months in the year they dominantly occur. This was done based on similarities in atmospheric patterns and seasonal frequency from the 3 X 3 node SOM. These nodes are hereafter referred to as nodes one (1) to six (6). The SOM nodes are noted to generally represent patterns of the seasonal cycle of monthly rainfall amounts. Circulation patterns in node 1 can be attributed to cases primarily observed in the first three months (January, February, and March) and the last two months (November, and December), hence a pattern most representative of the dry season months. It is noted that nodes 2 and 3 depict an environment that is prominent during the pre-monsoon season, with node 2 presenting a clearer seasonal exclusivity while node 3 shows frequent occurrences throughout the monsoon season. Patterns of node cases significant in the post-monsoon season are observed in nodes 4 and 5. However, node 4 evidently shows transition patterns that have frequent occurrences in both pre and post-monsoon seasons although most prominent in the post-monsoon season. Patterns in node 6 are more strongly related to peak monsoon conditions.

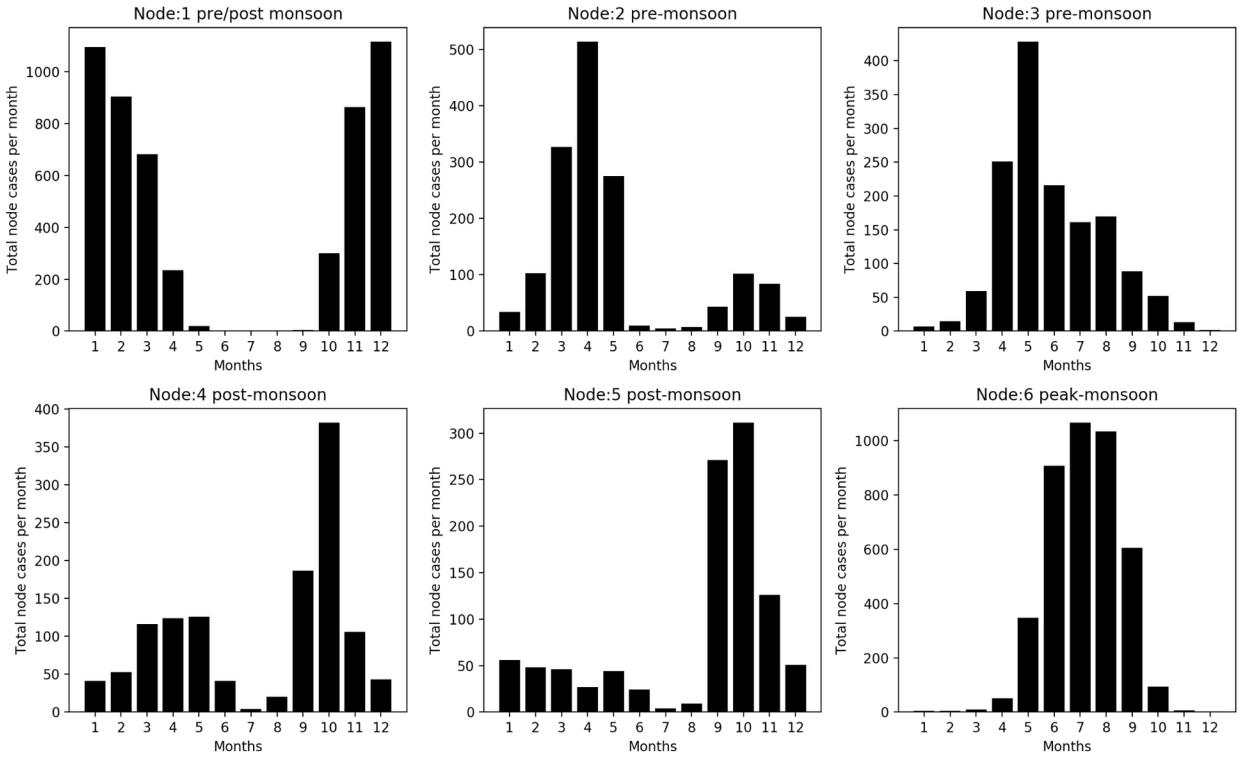

Figure 1. Monthly distribution of node cases based on SOM analysis

The SOM~~s~~ classification of different synoptic states was based on 925 hPa geopotential heights, with resulting patterns shown in Fig. 2. The patterns clearly show the signature of the well-known West African Heat Low (e.g. Lavaysse et al. 2009) moving northwards, strengthening over the course of the annual WAM cycle (from nodes 1, 2, and 3) and peaking in August, evident as an area of high pressure over the Sahara in node 6. Nodes 4 and 5 show stages of the weakening of the heat low post-monsoon, coinciding with a southward movement of the ~~650~~925 hPa high pressure area and linked southward retreat of mid-level easterly winds compared to node 6.

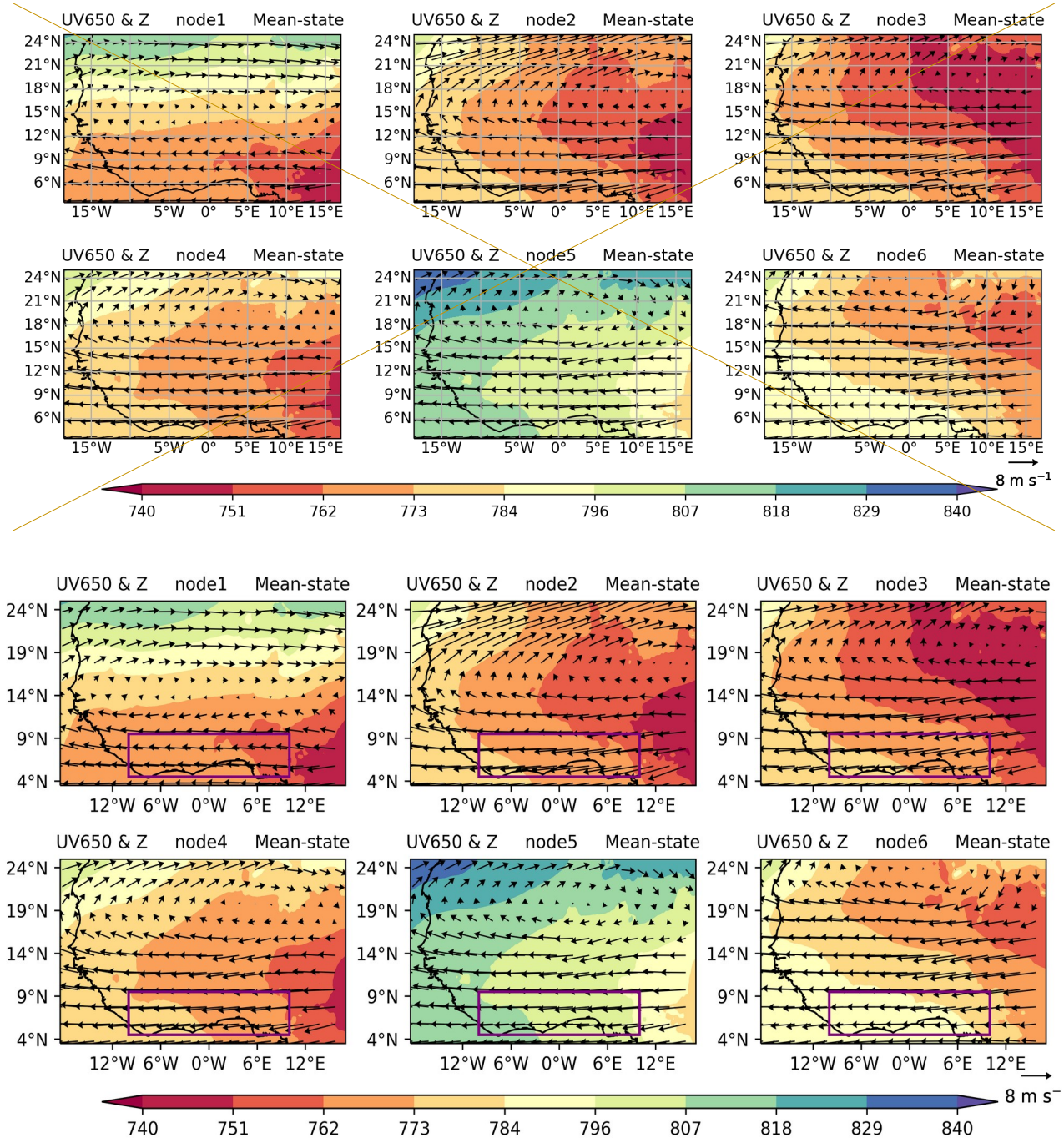

Figure 2. 12 UTC c~~C~~omposites of 925-hPa geopotential height (shading; gpm) and 650-hPa winds (vectors; m s^{-1}) in six nodes based on SOM analysis. The purple box depicts the SWA region (5°–9°N, 10°W–10°E)

We now examine surface winds and moisture flows to explore their behaviour under the six distinct circulation types identified (Fig. 3). In the first node, the north-easterly winds dominate most of West Africa, with weak southerlies over SWA. This pattern in moisture distribution is evident in the dry season over West Africa,

signaling a low moisture presence. The enhanced moisture observed in coastal areas of SWA can be attributed to the penetration of southerly winds. In pre-monsoon node 2, the southerly winds strengthen and move inland, causing the north-easterly winds to retreat. A similar effect is observed in nodes 3, 4, and 5 where the north-easterlies become weaker. In node 6, the south-westerlies are ~~much more strengthened~~intensified and move inland, further enhancing moisture flow from the South Atlantic towards the land, representative of peak monsoon flow. Wind patterns for low- and mid-levels (Figs. 2 and 3) illustrate vertically-sheared conditions coinciding with regions of high low-level specific humidity in all nodes (purple in Fig. 3), thus marking regions where atmospheric conditions may allow MCS development.

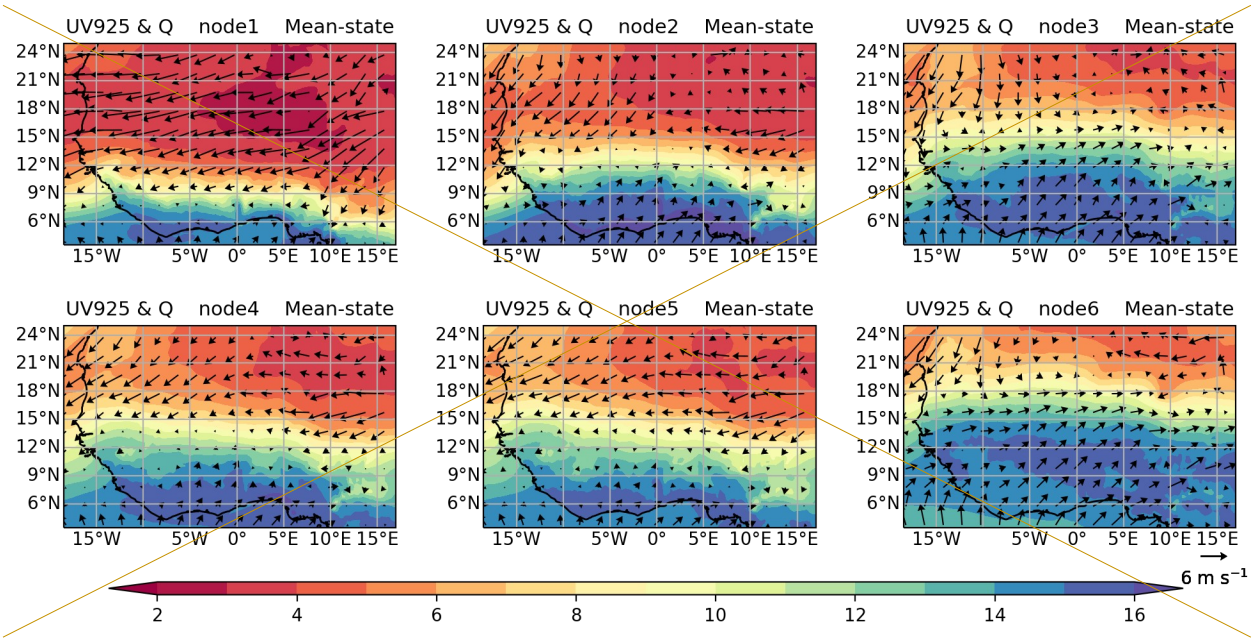

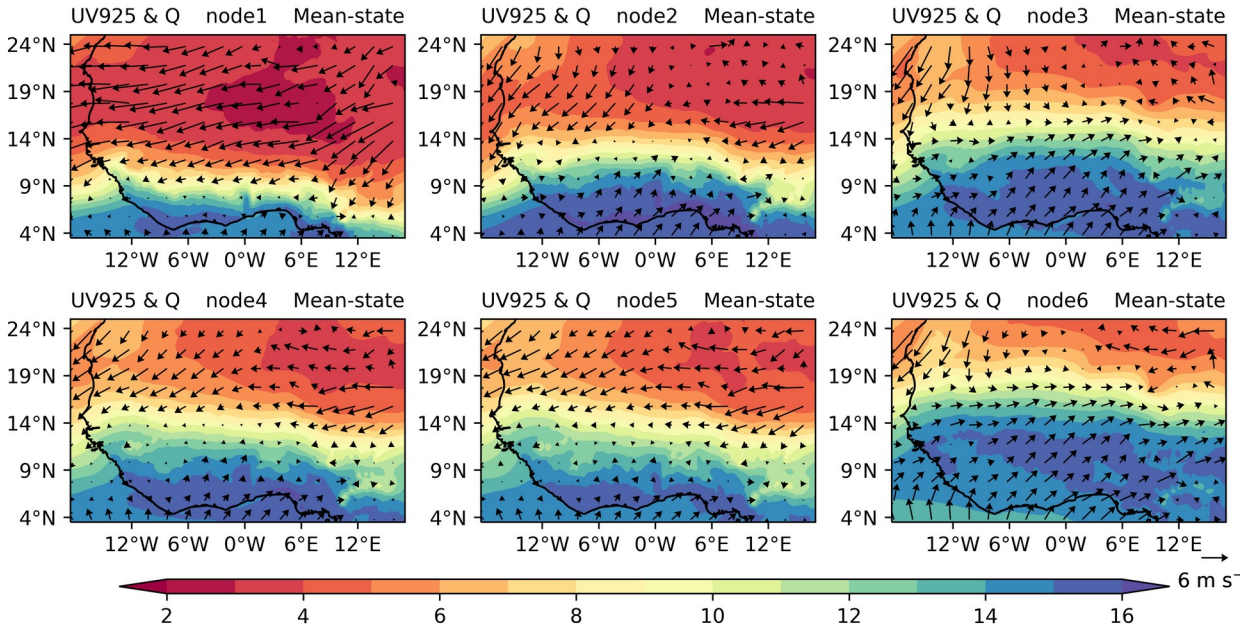

Figure 3. 12 UTC c~~C~~omposites of specific humidity (shading; g kg^{-1}) and 925-hPa winds (vectors; m s^{-1}) in six nodes based on SOM analysis.

A further investigation was conducted to ascertain the spatial distribution of mean zonal wind shear over SWA (Fig. 4). The patterns demonstrate northward transport during the propagation of the WAM cycle and a wider spread of zonal wind shear as it moves further inland (nodes 1, 2, and 3). These patterns closely follow the southern boundary of weaker geopotential heights representative of high-pressure areas (Fig. 2). During the monsoon season (node 6), zonal wind shear lies clearly to the north of the SWA domain. A southward retreat of zonal wind shear is observed during the post-monsoon season (nodes 4 and 5). Generally, the presence of zonal wind shear can be seen as a necessary condition in the WAM system.

~~A further investigation into potential node frequency trends since the 1980s was conducted to ascertain whether certain node frequencies have changed over recent years (Fig. 4). No clear node frequency changes are observed during nodes associated with the dry and the monsoon seasons (node 1, 6). It is also striking that the two nodes associated with the second rainy season months (node 4, 5) show significant changes (p-value < 0.05) over the 4 last decades, indicating that this season may have been affected by long-term changes in the large-scale environment, although node 5 recovered in the last few years. But it would have to be investigated in more detail when exactly these trends occur and which variables are affected, which is out of scope of this study.~~

~~**Figure 4.** Time series of node frequency trends for node climatologies over the years. Deep blue line indicates 5-year rolling mean of node frequencies. The titles show the mann kendall trend test and the p-value for test of significance.~~

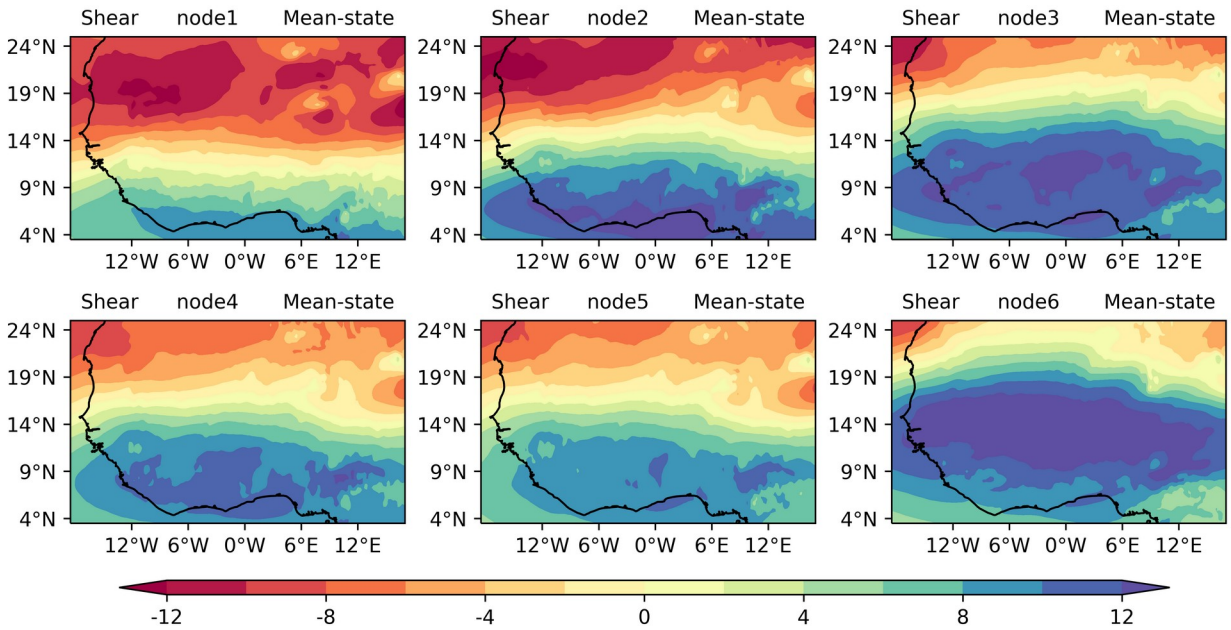

Figure 4. 12 UTC composites of zonal wind shear in six nodes based on SOM analysis.

4.2 Large-scale conditions favouring MCS days

The environmental conditions favouring MCS occurrence are described in this section. Firstly, the monthly climatology of MCS frequency as captured by our MCS snapshots (average number of MCSs at 1800 UTC across SWA domain) is considered with a focus on rainfall months. A pronounced annual cycle of MCS numbers with frequency peaks in June and September is observed (Fig. 5). These peak months are associated with maximum rainfall during the major and minor rainy seasons across SWA respectively. The monthly climatology of MCS frequency decreases from June to August, with August being the local minimum. This local minimum corresponds to the so-called “little dry season” (Le Barbé et al., 2002; Vollmert et al., 2003) that exists before the southward retreat of the rainbelt.

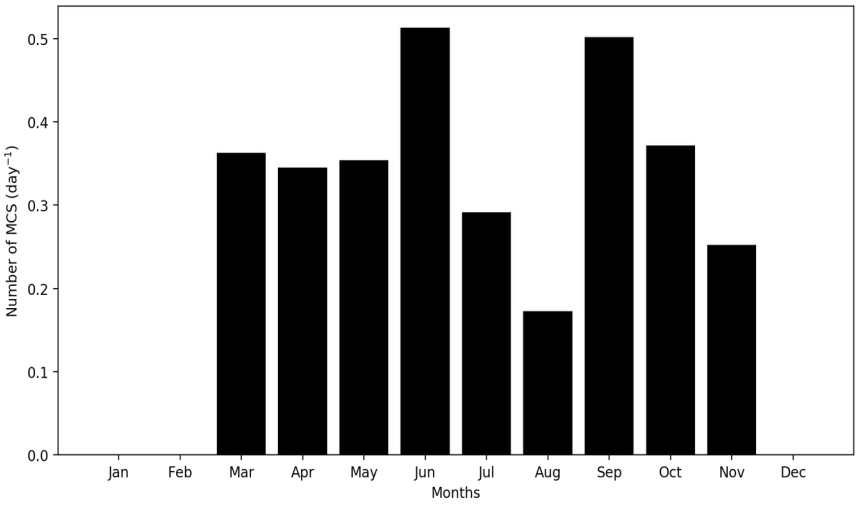

277 **Figure 5.** Average annual cycle of MCSs at 1800 UTC within the SWA box showing the monthly average of MCS
278 number per day.
279
280

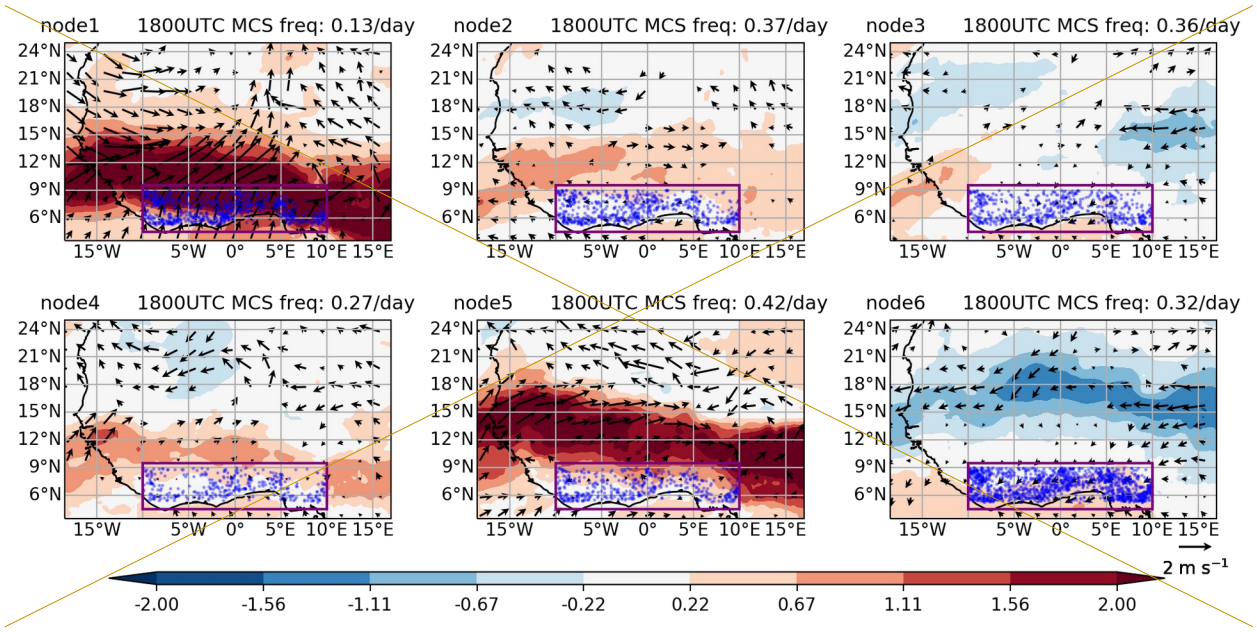

281

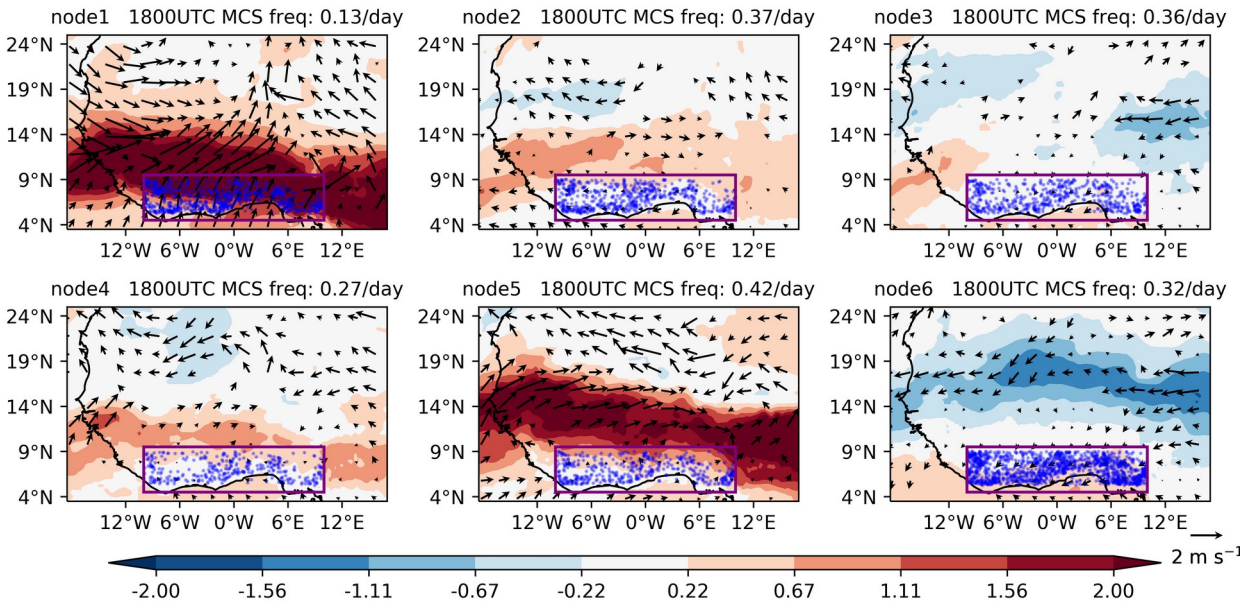

Figure 6. 12 UTC MCS-day composite anomalies of specific humidity (shading; g kg^{-1}) and 925-hPa winds (vectors; m s^{-1}) in six nodes based on SOM analysis. The purple box depicts the SWA region (5°–9°N, 10°W–10°E) and the blue dots indicate the location of MCSs during node days. Specific humidity anomalies are shown when they are significant at the 5% level; wind vectors are shown when either the zonal or meridional wind anomalies are significant at the 5% level.

~~We consider the spatial distribution of large-scale environments associated with MCSs for each node over the SWA region.~~ In node 1, a positive widespread moisture anomaly maximum is observed with anomalous south-westerly winds over SWA (Fig. 6). This depicts a substantial enhancement in the low-level moisture transport during days of convective activities. In nodes 2, 3, 4, and 5, low-level moisture anomalies during convective activity days show insignificant behaviour along the SWA coast based on the two-sided Student's t-test. In node 5, a positive moisture anomaly is located over the northern part of SWA. In node 6, a notable region of anomalous easterly winds and also the seemingly partly northerlies from the Mediterranean region coincides with negative moisture anomalies over the Sahel. Strong easterly winds during MCS days reduce the moisture over the Sahel but introduce more moisture over the coast. Comparing daily MCS frequencies, we find that MCSs are most likely to develop under node 5 conditions featuring a northward-displaced moisture anomaly (0.42 MCSs per day), linked to strengthened low-level westerlies. Given this node occurs predominantly from September and into November - the minor rainy season in SWA (cf. Fig.~1), these patterns may in some cases be representative of a delayed monsoon retreat.

Figure 7 shows a widespread increase in temperature north of SWA during days with active convection in nodes 1, 2, 4, and 5. The SWA region itself reveals a negative and/or insignificant change in temperature during MCS days when compared with the mean climatology. ~~This could be a result of the presence of enhanced moisture migrating from the Atlantic ocean inland (Fig. 6).~~ Indeed, for nodes 1 and 5 this coincides with low-level westerly wind south of 15N (cf. Fig. 6). In node 6, temperatures are enhanced in most parts of West Africa including SWA.

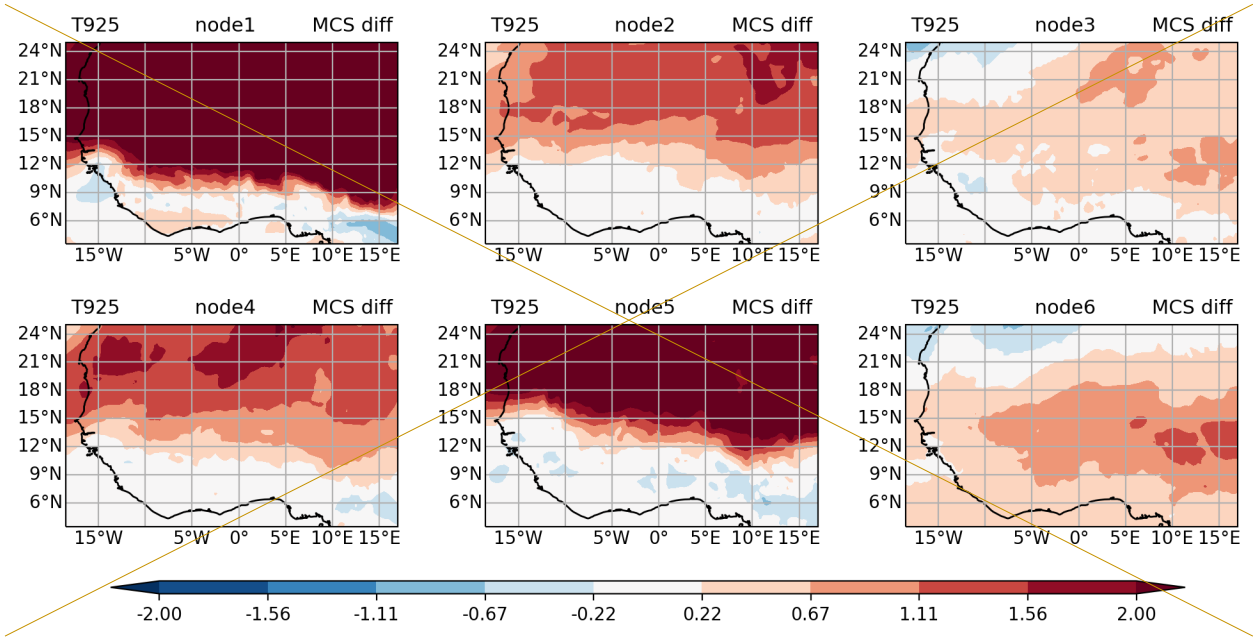

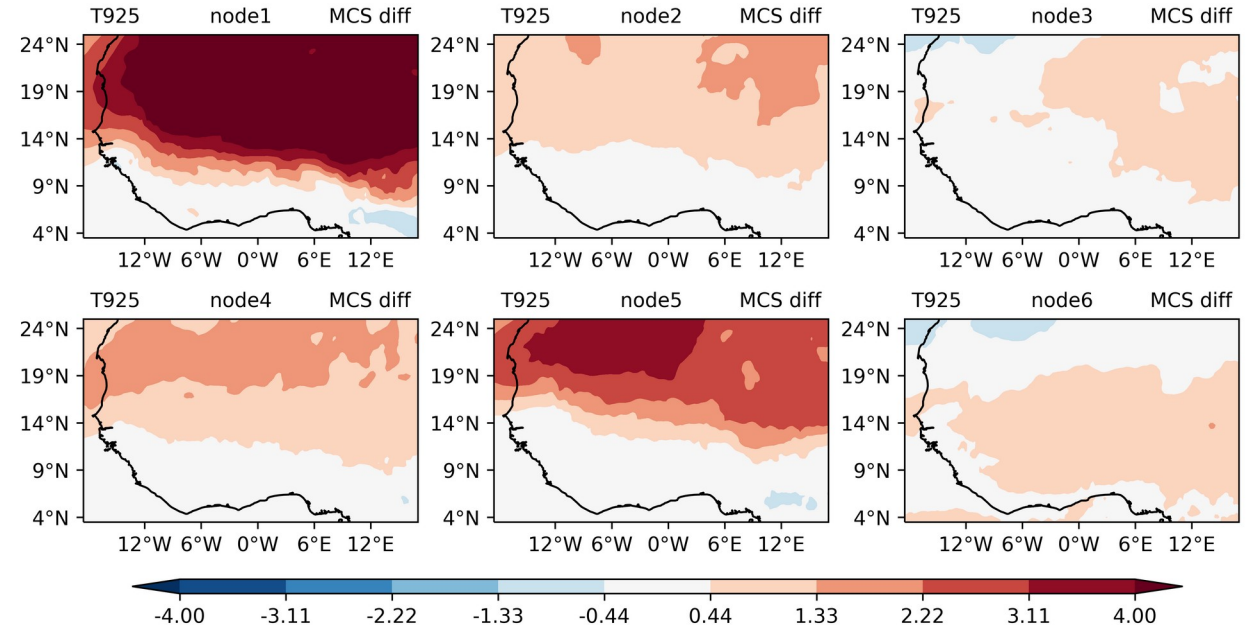

Figure 7. 12 UTC cComposite anomalies of 925hPa temperatures (°C) in six nodes based on SOM analysis. Temperature anomalies are shown when they are significant at the 5% level.

Figure 8 shows the spatial distribution of zonal wind shear anomaly between days with convective MCSs over SWA and the climatological zonal wind shear mean for the 6 different nodes across West Africa. Generally, all nodes except node 6, reveal a widespread increase in zonal wind shear anomaly over West Africa with nodes 1 and 5 depicting stronger events. WZonal wind shear tends to be stronger during the dry and early part of the major rainy

season (node 1) with its peak partly over SWA, but resides to the north of SWA during the minor rainy season (nodes 4 and 5), in line with previously identified zonal wind shear seasonality for the region (Klein et al. 2021). Nodes 4 and 5 (post-monsoon) however still experience an appreciably significant increase in zonal wind shear over SWA for MCS days during the minor rainy season. Node 6 on the other hand, ~~observe~~exhibits a significant increase in zonal wind shear mainly confined to SWA. In line with the expected zonal wind shear response to an increased large-scale meridional temperature gradient, we find strongest zonal wind shear anomalies for nodes with strongest low-level temperature anomalies to the north of SWA (nodes 1,5; followed by nodes 2,4), highlighting that a warmer Sahel can promote MCS-favourable conditions in SWA, particularly in the pre- and post-monsoon seasons. ~~Overall, these significant positive zonal shear anomalies for MCS days across all nodes illustrate the importance of shear for MCS development in SWA throughout the year.~~

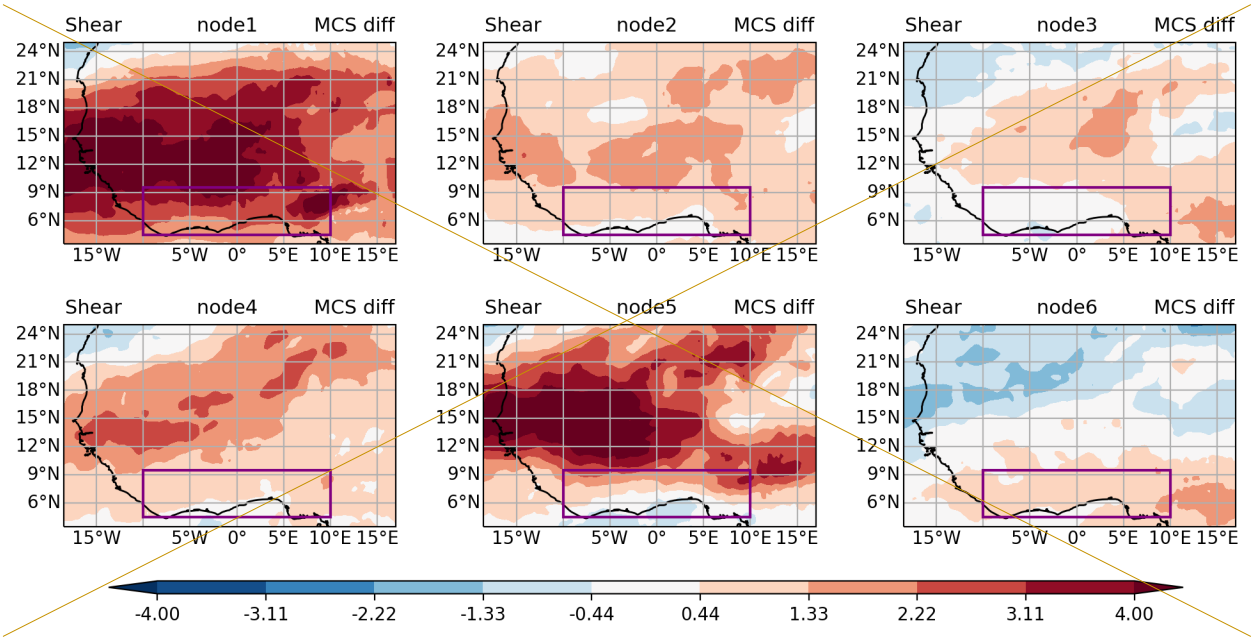

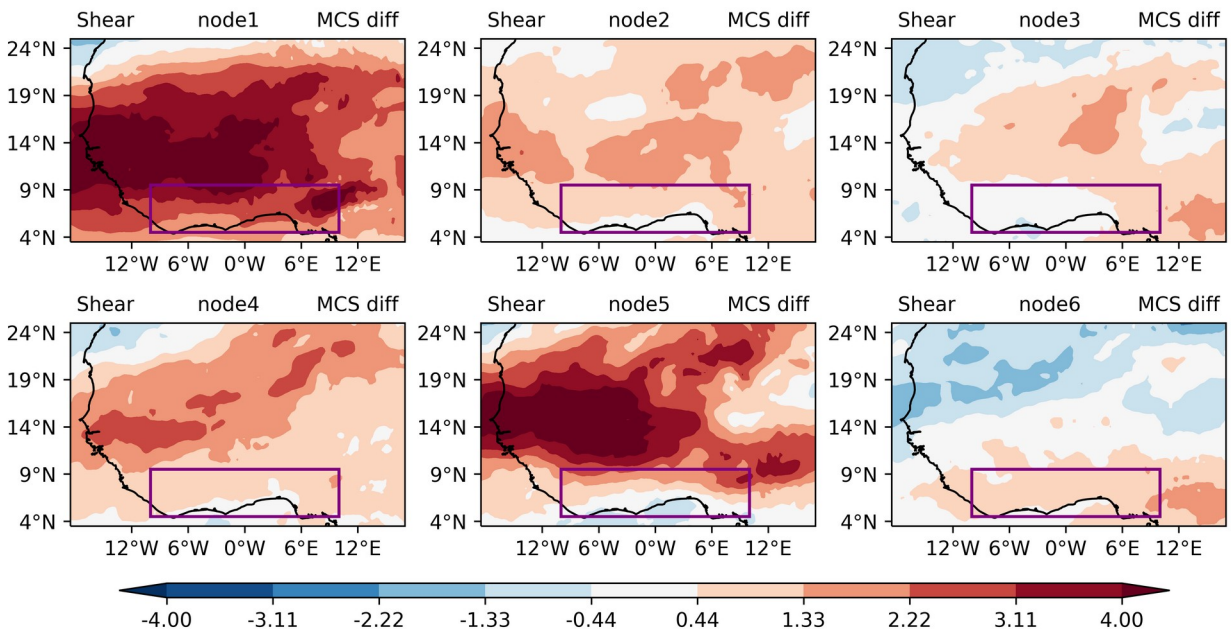

Figure 8. 12 UTC c~~C~~omposite anomalies of zonal wind shear (m s^{-1}) in six nodes based on SOM analysis. ~~S~~zonal wind shear anomalies are shown when they are significant at the 5% level.

Investigating the first order condition for convection development, we also evaluate CAPE for a parcel at 925 hPa to ascertain the level of increased MCS-day instability in various nodes over SWA (Fig. 9). A large strip of higher CAPE values extending over the entire region of SWA and the southern Sahel from 5°N−15°N is observed (node 1). This large strip of higher CAPE is situated further north of SWA for node 5, while part of the western coast tends to ~~observe~~depict patterns of lower CAPE values, suggesting increased MCS likelihood only for eastern parts of the domain. Node 3 shows a swath of high CAPE values in particular to the east and in some instances extends to the central (node 4) and south-western parts of SWA (node 6). For nodes 3-6, higher CAPE conditions over SWA are to differing degrees significantly associated with decreased CAPE in the Sahelian region, creating a dipole pattern that can occur during pre-, peak- and post-monsoon periods according to node frequencies (cf. Fig 1). Overall, all nodes show positive CAPE anomalies for MCS-days in parts of SWA, creating an environment sufficiently unstable to support the development of convection. It can be said that regions over SWA that exhibit a higher CAPE on MCS days also depict stronger zonal wind shear (Fig. 8). Indeed, it has previously been shown that colder, more intense MCSs predominantly occur under conditions with high CAPE and high zonal wind shear anomalies (Klein et al, 2021), which we show is consistent across all classified large scale patterns.

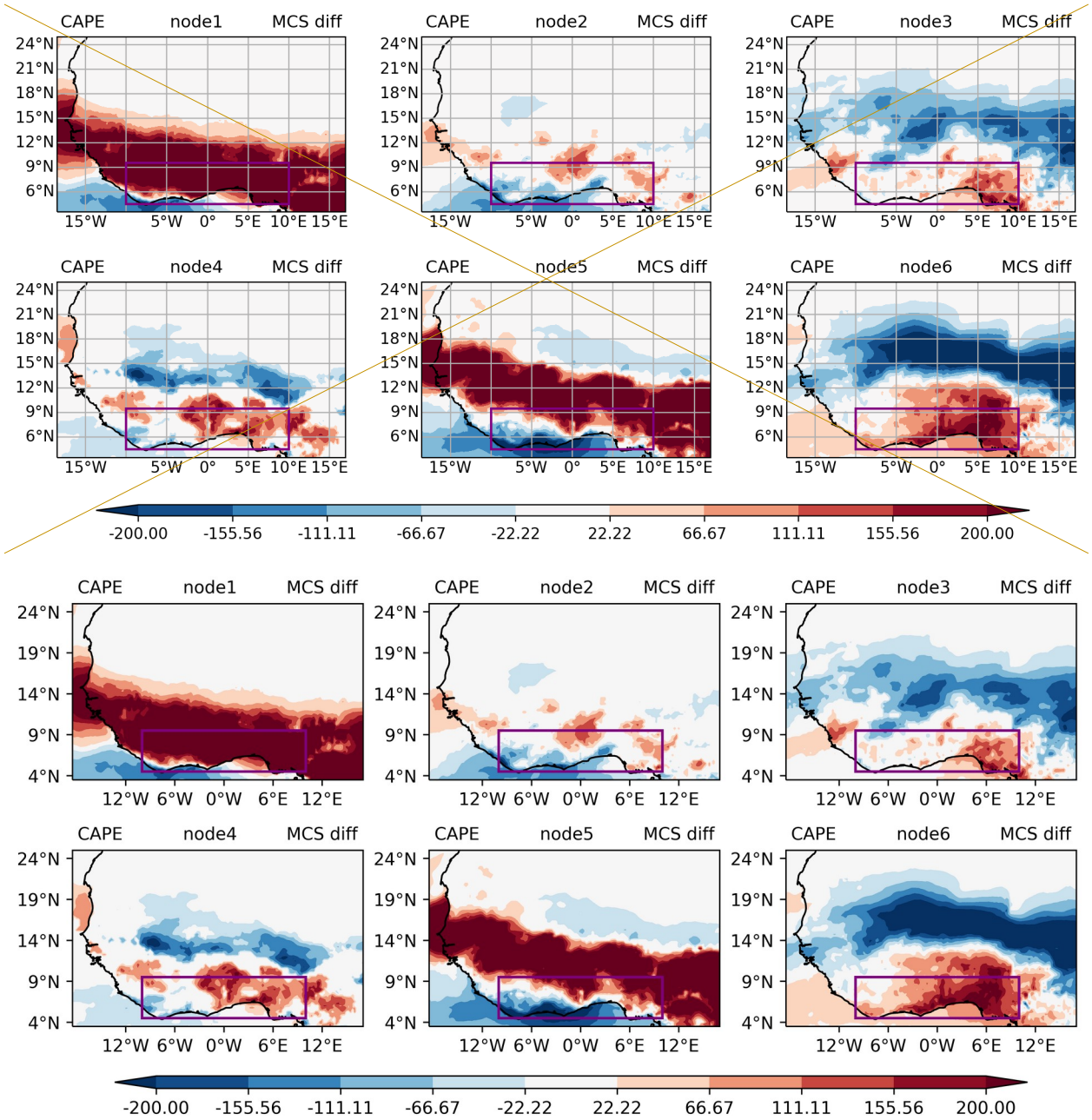

Figure 9. 12 UTC cComposite anomalies of CAPE (J kg^{-1}) for MCSs occurring in each type of large-scale environment determined by the SOM analysis over SWA. CAPE anomalies are shown when they are significant at the 5% level.

4.3 MCS driver variability within nodes

The drivers of MCSs within different nodes are considered to examine their relative importance within the different large-scale states (Fig. 10), concentrating on total column water vapor (TCWV) and zonal wind shear. Node 1 climatological conditions depict both, a very low initial zonal wind shear and TCWV., This illustratinges the relatively low storm hostile conditions during mean conditions for this node, predominantly representing dry season

conditions and explaining the low storm frequency of only 0.13 per day (cf. Fig. 6). Interestingly, on storm days, conditions for this node shift to within the range of environmental conditions identified for other nodes with higher storm frequencies, albeit node 6 MCS-day conditions still represent the lowest values in TCWV and zonal wind shear.

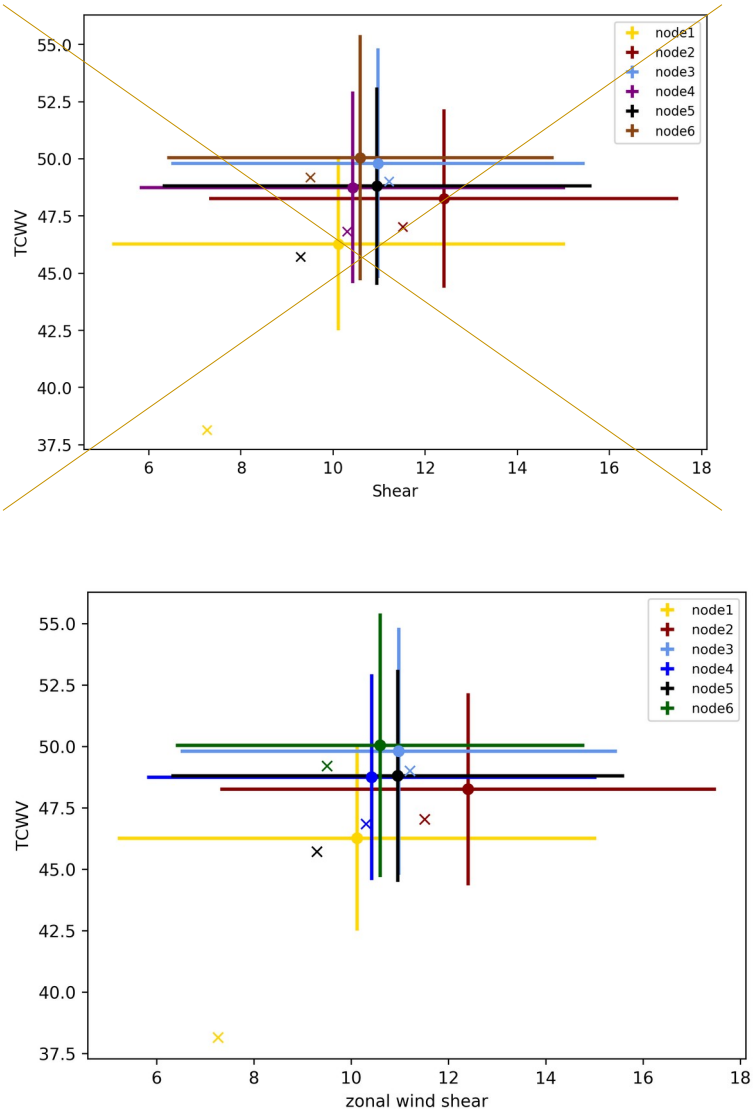

Figure 10. Mean MCS conditions over SWA for the different nodes. Dots show the mean within 1 standard deviation (whiskers) across each node. The symbol (x) denotes the mean environmental condition for all node days (MCS and non-MCS).

Pre-monsoon nodes (nodes 2 and 3) observe initial higher zonal wind shear conditions than all other nodes with appreciably higher TCWV. Node 2 observes an increase in zonal wind shear (about 1 m/s) and also a bit more

TCWV. Not much change is observed in the zonal wind shear and TCWV value for node 3, making node 2 the season with relatively strong instability~~. since this node (node 2)~~. Comparing nodes 4 and 5 (both post-monsoon nodes), it can be observed that node 5 has lower zonal wind shear to start with and thus needs higher zonal wind shear change to produce MCS conditions very similar to node 4. Node 4 on the other hand shows mostly TCWV change but has a bit more zonal wind shear so, in spite of the smaller zonal wind shear anomaly (Fig. ~~8~~7), the resulting MCS conditions are rather similar. Node 6 depicts an initial environmental condition of high TCWV over SWA, which is typical of periods with frequent convective activities during peak monsoon. During MCS events, there is a slight increase in zonal wind shear (about 1 m/s) and TCWV (about 0.8 kg/m^2), depicting more convective activities during th~~is~~e monsoon season.

Generally, it can be noted that all nodes show increased TCWV on MCS days compared to their climatology. The smallest changes for both TCWV and zonal wind shear between climatology and MCS day occur for node 3, which shows the highest frequency for pre-monsoon transition month May but is still common throughout the monsoon season (c.f. Fig. 1) . Together with node 4, it is also the only node for which zonal wind shear conditions remain approximately similar, but with climatological zonal wind shear strengths already reaching > 10 m~~-~~/s at MCS location. Overall, node environmental conditions become more similar for MCS-days relative to the climatologies, illustrating that favourable MCS conditions converge towards high TCWV (affecting CAPE), and high zonal wind shear environments irrespective of the large-scale situation.

5 Conclusion

The study identified six synoptic states ~~(pure node analysis)~~ and then examined what changes are associated with favourable MCS environments in Southern West Africa under these states. For the definition of synoptic states and MCS days, we used self-organizing maps (SOM) based on ERA5 geopotential height data and 12 years of tracked MCSs using Meteosat Second Generation (MSG) 10.8 μm-band brightness temperature data (2004-15), respectively. The identified synoptic states based on the SOM nodes are noted to generally represent patterns of the seasonal rainfall cycle. Circulation patterns in node 1 can be attributed to cases primarily observed in the dry season months (January, February, November, and December). An environment representative of the pre-monsoon season is depicted by nodes 2 and 3, with node 2 presenting a clearer seasonal exclusivity. Patterns of the post-monsoon season are observed in nodes 4 and 5 with node 4 evidently depicting transition patterns that have frequent occurrences in both pre and post-monsoon seasons although prominent in the post-monsoon season. Peak monsoon conditions are clearly represented in node 6 with large-scale conditions occurring mainly in June, July, and August. The south-westerly winds observed over SWA are strengthened and move inland, enhancing moisture flow from the South Atlantic towards the land during the peak monsoon. In the pre-monsoon and post-monsoon seasons, similar but weakened south-westerly circulation patterns are observed. The synoptic-state-related MCSs realize a pronounced annual cycle of MCS numbers with frequency peaks in June and September. These peak months are well associated with maximum rainfall during the major and minor rainy seasons across SWA respectively. During the course of the year, MCSs are most likely to develop under post-monsoon conditions featuring a northward-displaced moisture anomaly (0.42 MCSs per day) which is associated with strengthened low-level westerlies, and in

some cases may be representative of a delayed monsoon retreat. Furthermore, the strongest zonal wind shear anomalies over SWA are realized in seasons with the strongest low-level temperature anomalies to the north of SWA, representative of favourable MCS conditions in SWA during periods of a warmer Sahel. Regions over SWA that show stronger zonal wind shear on MCS days also depict higher CAPE. We found node environmental conditions to become more similar for MCS-days relative to the node climatologies, illustrating that favourable MCS conditions converge towards high TCWV/high zonal wind shear states. Overall, our results show that MCSs develop on average in similar high moisture, high zonal wind shear local environments under all large-scale situations throughout the year. The latter however defines the frequency at which favourable MCS environments can occur.

Code and data availability. Codes for the findings of this study are available upon reasonable request from the authors. The processing of ERA5 data made direct access to the primary data archive held at ECMWF, and is available from the Copernicus Data Store (https://cds.climate.copernicus.eu/) and the MSG data are available from http://www.eumetsat.int.

Author contributions. FN, NABK and CK conceptualized the study, with input from KAQ; All authors contributed to and discussed the methodological design, and analyses were conducted by FN and CK; FN, ROB and KAQ wrote the manuscript draft; CK, NABK, PE, GMLDQ and HAK reviewed and edited the manuscript.

Competing interests. The contact author has declared that none of the authors has any competing interests.

Acknowledgments. This work is supported by a grant from the Government of Canada, provided through Global Affairs Canada, www.international.gc.ca (accessed on 1 January 2021), and the International Development Research Centre, www.idrc.ca, (accessed on 1 June 2022) to the African Institute for Mathematical Sciences—Next Einstein Initiative (AIMS-NEI) [Number: 108246-001]. CK acknowledges funding from the NERC-funded LMCS project (NE/W001888/1). KQ also acknowledges funding from the National Research Foundation (NRF), South Africa.

References

Alfaro, D. A.: Low-Tropospheric Shear in the Structure of Squall Lines: Impacts on Latent Heating under Layer-Lifting Ascent, J Atmos Sci., 74, 229–48, https://doi.org/10.1175/JAS-D-16-0168.1, 2017.

Augustin, D., Pascal, I.M., Jores, T.K., Elisabeth, F.D., Cesar, M.B., Michael, T.F., Roméo-Ledoux, D.T., Marceline, M., Gladys, K.N.F. and Firmin, B.A.: Impact Assessment of the West African Monsoon on Convective Precipitations over the Far North Region of Cameroon, Adv. Space Res., https://doi.org/10.1016/j.asr.2022.04.044, 2022.

Baidu, M., Schwendike, J., Marsham, J.H. and Bain, C.: Effects of Vertical Wind Shear on Intensities of Mesoscale Convective Systems over West and Central Africa, Atmos. Sci. Lett, e1094, https://doi.org/10.1002/asl.1094, 2022.

Biasutti, M., Sobel, A. H., & Camargo, S. J.: The role of the Sahara low in summertime Sahel rainfall variability and change in the CMIP3 models. Journal of Climate, 22(21), 5755-5771, https://doi.org/10.1175/2009JCLI2969.1, 2009.

Cassano, E.N., Glisan, J.M., Cassano, J.J., Gutowski Jr, W.J. and Seefeldt, M.W.: Self-Organizing Map Analysis of Widespread Temperature Extremes in Alaska and Canada, Clim. Res. 62, 199-218, https://doi.org/10.3354/cr01274, 2015.

Chen, Y., Luo, Y. and Liu, B.: General Features and Synoptic-Scale Environments of Mesoscale Convective Systems over South China during the 2013-2017 Pre-Summer Rainy Seasons, Atmos. Res., 266, https://doi.org/10.1016/j.atmosres.2021.105954, 2022.

Feng, Z., Leung, L.R., Liu, N., Wang, J., Houze Jr, R.A., Li, J., Hardin, J.C., Chen, D. and Guo, J. A.: Global High-Resolution Mesoscale Convective System Database Using Satellite-Derived Cloud Tops, Surface Precipitation, and Tracking, J. Geophys. Res. Atmos. 126, e2020JD034202, https://doi.org/10.1029/2020JD034202, 2021.

Guo, Y., Du, Y., Lu, R., Feng, X., Li, J., Zhang, Y. and Mai, Z.: The Characteristics of Mesoscale Convective Systems Generated over the Yunnan-Guizhou Plateau during the Warm Seasons, Int. J. Climatol., http://doi.org/10.1002/joc.7647, 2022.

Guy, N., Rutledge, S.A. and Cifelli, R.: "Radar Characteristics of Continental, Coastal, and Maritime Convection Observed during AMMA/NAMMA", Q. J. R. Meteorol. Soc. 137, 1241-56, http://doi.org/10.1002/qj.839, 2011.

Hewitson, B. C., & Crane, R. G.: Climate Downscaling: Techniques and Application. Clim. Res. 7, 85-95, https://doi.org/10.3354/cr007085, (1996).

Hewitson, B. C., & Crane, R. G. "Self-Organizing Maps: Applications to Synoptic Climatology." Clim. Res. 22, 13-26, https://doi:10.3354/cr022013, (2002).

Hodges, K.I. and Thorncroft, C.D.: Distribution and Statistics of African Mesoscale Convective Weather Systems Based on the ISCCP Meteosat Imagery, Mon Weather Rev 125, 2821-37, https://doi.org/10.1175/1520-0493(1997)125<2821:DASOAM>2.0.CO;2, 1997.

Houze Jr, Robert A.: Mesoscale Convective Systems", Rev. Geophys., 42, http://doi:10.1029/ 2004RG000150, 2004.

Hussain, M.S., Kim, S. and Lee, S.: On the Relationship between Indian Ocean Dipole Events and the Precipitation of Pakistan, Theor. Appl. Climatol. 130, 673-85, http://doi.org/10.1007/s00704-016-1902-y, 2017.

IPCC: Climate Change, 2014: Synthesis Report. Contribution of Working groups I, II, and III to the Fifth Assessment Report of the Intergovernmental Panel on Climate Change [Core Working Team, R.K. Pachauri and L.A. Meyer (eds)]. IPCC, Geneva, Switzerland, 151, 2014

Janiga, M.A. and Thorncroft, C.D.: The Influence of African Easterly Waves on Convection over Tropical Africa and the East Atlantic, Mon Weather Rev 144, 171-92, https://doi.org/10.1175/MWR-D-14-00419.1, 2016.

Kamara, S. I.: The Origins and Types of Rainfall in West Africa, Weather 41, 48-56, https://doi.org/10.1002/j.1477-8696.1986.tb03787.x, 1986.

Kim, H.K. and Seo, K.H.: Cluster Analysis of Tropical Cyclone Tracks over the Western North Pacific Using a Self-Organizing Map, JCLI 29, 3731-51, https://doi.org/10.1175/JCLI-D-15-0380.1, 2016.

Klein, C., Belušić, D., & Taylor, C. M.: Wavelet scale analysis of mesoscale convective systems for detecting deep convection from infrared imagery.Journal of Geophysical Research: Atmospheres, 123, 3035 - 3050. https://doi.org/10.1002/2017JD027432, 2018.

Klein, C., Nkrumah, F., Taylor, C.M. and Adefisan, E.A.: Seasonality and Trends of Drivers of Mesoscale Convective Systems in Southern West Africa, JCLI 34, 71-87, https://doi.org/10.1175/JCLI-D-20-0194.1, 2021.

Kohonen, T. "Self-Organizing Maps.-Springer Series in Information Sciences, V. 30, Springer Sci. Rev., https://doi.org/10.1007/978-3-642-56927-2, 2001.

Kusangaya, S., Warburton, M.L., Van Garderen, E.A. and Jewitt, G.P.: Impacts of Climate Change on Water Resources in Southern Africa: A Review, Phys. Chem. Earth., 47-54, https://doi.org/10.1016/j.pce.2013.09.014, 2014.

Laing, A.G., Carbone, R., Levizzani, V. and Tuttle, J.: The Propagation and Diurnal Cycles of Deep Convection in Northern Tropical Africa, Q J R Meteorol Soc. 134, 93-109, http://doi.org/10.1002/qj.194, 2008.

Lavaysse, C., Flamant, C., Janicot, S., Parker, D.J., Lafore, J.P., Sultan, B. and Pelon, J.: Seasonal Evolution of the West African Heat Low: A Climatological Perspective, Clim. Dyn. 33, 313-30, https://doi.org/10.1007/s00382-009-0553-4, 2009.

Le Barbé, L., Lebel, T., & Tapsoba, D.: Rainfall variability in West Africa during the years 1950 - 90. J. Clim. 15(2), 187-202, https://doi.org/10.1175/1520-0442(2002)015<0187:RVIWAD>2.0. CO;2, 2002.

Li, P., Moseley, C., Prein, A.F., Chen, H., Li, J., Furtado, K. and Zhou, T.: Mesoscale Convective System Precipitation Characteristics over East Asia. Part I: Regional Differences and Seasonal Variations, J. Clim. 33, 9271-86, https://doi.org/10.1175/JCLI-D-20-0072.1, 2020.

Maranan, M., Fink, A.H. and Knippertz, P.: Rainfall Types over Southern West Africa: Objective Identification, Climatology and Synoptic Environment, Q J R Meteorol Soc. 144, 1628-48, https://doi.org/10.1002/qj.3345, 2018.

Mohr, K. I., and Zipser, E. J.: Mesoscale convective systems defined by their 85-GHz ice scattering signature: Size and intensity comparison over tropical oceans and continents. *Mon. Wea. Rev.*, 124, 2417-2437, https://doi:10.1175/1520-0493(1996)124<2417:MCSDBT>2.0.CO;2, 1996

Mohr, K.I. and Thorncroft, C.D.: Intense Convective Systems in West Africa and Their Relationship to the African Easterly Jet, Q J R Meteorol Soc. 132, 163-76, https://doi.org/10.1256/qj.05.55, 2006.

Nesbitt, S.W., Cifelli, R. and Rutledge, S.A.: Storm Morphology and Rainfall Characteristics of TRMM Precipitation Features, Mon Weather Rev 134, 2702-21, https://doi.org/10.1175/MWR3200.1, 2006.

Queralt, S., Hernández, E., Barriopedro, D., Gallego, D., Ribera, P. and Casanova, C.: North Atlantic Oscillation Influence and Weather Types Associated with Winter Total and Extreme Precipitation Events in Spain, Atmos. Res. 94, 675-83, https://doi.org/10.1016/j.atmosres.2009. 09.005, 2009.

Schmetz, J., Pili, P., Tjemkes, S., Just, D., Kerkmann, J., Rota, S. and Ratier, A.: An Introduction to Meteosat Second Generation (MSG)", Bull Am Meteorol Soc 83, 977-92, https://doi.org/10.1175/1520-0477(2002)083<0977:AITMSG>2.3.CO;2, 2002.

Schrage, J.M., Fink, A.H., Ermert, V. and Ahlonsou, E.D.: Three MCS Cases Occurring in Different Synoptic Environments in the Sub-Sahelian Wet Zone during the 2002 West African Monsoon, J Atmos Sci 63, 2369-82, https://doi.org/10.1175/JAS3757.1, 2006.

Sheridan, S. and Lee, C.C.: Synoptic Climatology and the Analysis of Atmospheric Teleconnections, Prog Phys Geogr. 36, 548-57, https://doi/org/10.1177/0309133312447935, 2012.

Sultan, B., & Janicot, S.: The West African monsoon dynamics. Part II: The "preonset" and "onset" of the summer monsoon. Journal of climate, 16(21), 3407-3427, https://doi.org/10.1175/1520-0442(2003)016<3407:TWAMDP>2.0.CO;2, 2003.

Taylor, C.M., Belušić, D., Guichard, F., Parker, D.J., Vischel, T., Bock, O., Harris, P.P., Janicot, S., Klein, C. and Panthou, G.: Frequency of Extreme Sahelian Storms Tripled since 1982 in Satellite Observations, Nature 544, 475-78, https://doi.org/10.1038/nature22069, 2017.

Thorncroft, Chris D, Hanh Nguyen, Chidong Zhang, and Philippe Peyrillé.: Annual Cycle of the West African Monsoon: Regional Circulations and Associated Water Vapour Transport, Q. J. R. Meteorol. Soc. 137, 129-47, https//doi.org/10.1002/qj.728, 2011.

Vizy, E.K. and Cook, K.H.: Mesoscale Convective Systems and Nocturnal Rainfall over the West African Sahel: Role of the Inter-Tropical Front, Clim. Dyn. 50, 587-614, https://doi.org/10.1007/s00382-009-0553-4, 2018.

Wolski, P., Jack, C., Tadross, M., van Aardenne, L. and Lennard, C.: Interannual Rainfall Variability and SOM-Based Circulation Classification", Clim. Dyn. 50, 479-92, https://doi/org/10.1007/s00382 -017-3621-1, 2018.

~~Augustin, D., Pascal, I. M., Jores, T. K., Elisabeth, F. D., Cesar, M. B., Michael, T. F., ... & Firmin, B. A. (2022). Impact assessment of the West African monsoon on convective precipitations over the far north region of Cameroon. Advances in Space Research.~~

~~Baidu, M., Schwendike, J., Marsham, J. H., & Bain, C. (2022). Effects of vertical wind shear on intensities of mesoscale convective systems over West and Central Africa. Atmospheric Science Letters, e1094.~~

~~Bisselink, B., Zambrano-Bigiarini, M., Burek, P., & De Roo, A. (2016). Assessing the role of uncertain precipitation estimates on the robustness of hydrological model parameters under highly variable climate conditions. Journal of Hydrology: Regional Studies, 8, 112-129.~~

~~Cassano, E. N., J. M. Glisan, J. J. Cassano, W. J. Gutowski, and M. W. Seefeldt, 2015: Self-organizing map analysis of widespread temperature extremes in Alaska and Canada. Climate Res., 62, 199–218, https://doi.org/10.3354/cr01274~~

~~Chen, Y., Luo, Y., & Liu, B. (2022). General features and synoptic-scale environments of mesoscale convective systems over South China during the 2013–2017 pre-summer rainy seasons. Atmospheric Research, 266, 105954.~~

~~Feng, Z., Leung, L. R., Liu, N., Wang, J., Houze Jr, R. A., Li, J., ... & Guo, J. (2021). A global high-resolution mesoscale convective system database using satellite-derived cloud tops, surface precipitation, and tracking. Journal of Geophysical Research: Atmospheres,126(8), e2020JD034202.~~

Guo, Y., Du, Y., Lu, R., Feng, X., Li, J., Zhang, Y., & Mai, Z. (2022). The characteristics of mesoscale convective systems generated over the Yunnan-Guizhou Plateau during the warm seasons. International Journal of Climatology.

Hersbach, H., Bell, B., Berrisford, P., Hirahara, S., Horányi, A., Muñoz-Sabater, J., Nicolas, J., Peubey, C., Radu, R., Schepers, D., et al. (2020). The era5 global reanalysis. Quarterly Journal of the Royal Meteorological Society, 146(730):1999-2049.

Hewitson, B., and R. Crane, 1996: Climate downscaling: Techniques and application. Climate Res., 7, 85-95, https://doi.org/10.3354/cr007085.

Hewitson, B., and R. Crane, 2002: Self-organizing maps: Application to synoptic climatology. Climate Res., 22, 13-26, https://doi.org/10.3354/cr022013.

Houze Jr, R. A. (2004). Mesoscale convective systems. Reviews of Geophysics, 42(4).

Kim, H. K., and K. H. Seo, 2016: Cluster analysis of tropical cyclone tracks over the western North Pacific using a self-organizing map. J. Climate, 29, 3731–3751, https://doi.org/10.1175/JCLI-D-15-0380.1.

Klein, C., Nkrumah, F., Taylor, C. M., & Adefisan, E. A. (2021). Seasonality and trends of drivers of mesoscale convective systems in southern West Africa. Journal of Climate, 34(1), 71-87.

Kohonen, T., 1982: Self-organized formation of topologically correct feature maps. Biol. Cybern., 43, 59–69, https://doi.org/10.1007/BF00337288.

Kohonen, T., 2001: Self-Organizing Maps. Springer, 502 pp.

Kusangaya, S., Warburton, M. L., Van Garderen, E. A., & Jewitt, G. P. (2014). Impacts of climate change on water resources in southern Africa: A review. Physics and Chemistry of the Earth, Parts a/b/c, 67, 47-54.

Lavaysse, C., Flamant, C., Janicot, S., Parker, D. J., Lafore, J. P., Sultan, B. and Pelon, J.: Seasonal evolution of the West African heat low: A climatological perspective, Clim. Dyn., 33(2–3), 313–330, doi:10.1007/s00382-009-0553-4, 2009.

Lee, C. C., 2017: Reanalysing the impacts of atmospheric teleconnections on cold-season weather using multivariate surface weather types and self-organizing maps. Int. J. Climatol., 37, 3714–3730, https://doi.org/10.1002/joc.4950.

Lennard, C., and G. C. Hegerl, 2014: Relating changes in synoptic circulation to the surface rainfall response using self-organizing maps. Climate Dyn., 44, 861–879, https://doi.org/10.1007/s00382-014-2169-6.

Li, P., Moseley, C., Prein, A. F., Chen, H., Li, J., Furtado, K., & Zhou, T. (2020). Mesoscale convective system precipitation characteristics over East Asia. Part I: Regional differences and seasonal variations. Journal of Climate, 33(21), 9271-9286.

Maidment, R. I., Grimes, D., Allan, R. P., Tarnavsky, E., Stringer, M., Hewison, T., ... & Black, E. (2014). The 30 year TAMSAT African rainfall climatology and time series (TARCAT) data set. Journal of Geophysical Research: Atmospheres, 119(18), 10-619.

Maranan, M., Fink, A. H., & Knippertz, P. (2018). Rainfall types over southern West Africa: Objective identification, climatology and synoptic environment. Quarterly Journal of the Royal Meteorological Society, 144(714), 1628-1648.

Nesbitt, S. W., Cifelli, R., & Rutledge, S. A. (2006). Storm morphology and rainfall characteristics of TRMM precipitation features. Monthly Weather Review, 134(10), 2702-2721.

Quagraine, K. A., B. Hewitson, C. Jack, I. Pinto, and C. Lennard, 2019: A methodological approach to assess the co-behavior of climate processes over southern Africa. J. Climate, 32, 2483–2495, https://doi.org/10.1175/JCLI-D-18-0689.1

Sheridan, S., and C. C. Lee, 2012: Synoptic climatology and the analysis of atmospheric teleconnections. Prog. Phys. Geogr., 36, 548–557, https://doi.org/10.1177/0309133312447935.

Thorncroft, C. D., Nguyen, H., Zhang, C. and Peyrille, P., 2011: Annual cycle of the West African monsoon: Regional circulations and associated water vapour transport, Q. J. R. Meteorol. Soc., 137(654), 129–147, doi:10.1002/qj.728.

Wolski, P., C. Jack, M. Tadross, L. van Aardenne, and C. Lennard, 2018: Interannual rainfall variability and SOM-based circulation classification. Climate Dyn., 50, 479–492, https://doi.org/10.1007/s00382-017-3621-1.

645
646
647
648
649
650
651